Wind Velocity and Convergence Measurements at the Boulder Atmospheric Observatory Using Path-Averaged Optical Wind Sensors

MU-KING TSAY,[1] TING-I WANG, R. S. LAWRENCE, G. R. OCHS AND R. B. FRITZ

NOAA/ERL/Wave Propagation Laboratory, Boulder, CO 80303

(Manuscript received 17 October 1979, in final form 21 March 1980)

ABSTRACT

In a cooperative field study of the planetary boundary layer, three optical wind sensors were placed around a 300 m meteorological tower in a 450 m equilateral triangle 3–4 m above the terrain. It was found that the convergence measured by the three-sensor system correlates well with *in situ* measurements of vertical wind by anemometers located on the tower at heights up to 300 m during the occurrence of thermal plumes. By analyzing the correlation between the optically measured convergence and the vertical wind measurements made on the tower, the inversion layer, if below the top of the tower, can usually be located in the early morning when thermal plumes are active. The space-averaged horizontal wind vectors measured by the optical system have good, though not perfect, agreement with the tower measurements at the lowest layer (10 m above the ground), and with the measurements of a nearby network of surface anemometers. A comparison of the optically measured convergence with the direction of the surface horizontal wind indicates some effect of irregular terrain.

1. Introduction

Though it is difficult to measure, the convergence of the horizontal wind is an important quantity for meteorological studies. Many attempts have been made to develop methods based on point measurements (Bellamy, 1949; Morton *et al.*, 1956; Endlich and Clark, 1963; Eddy, 1964; Telford, 1966). Owing to a lack of suitable wind-measuring techniques, these have been difficult to check in the atmosphere. Kjelaas and Ochs (1974) successfully used three separate optical systems, each consisting of a 3 mW He-Ne laser, two photodiode receivers, and a small specialized data-processing circuit providing an output voltage proportional to path-averaged crosswind speed, to form an equilateral triangle, 300 m on a side and 2.3 m above the ground, to measure the divergence inside the triangle. For their experiments the terrain near the triangle was flat and free from any obstacles for a minimum of 3 km in any direction.

Recently, the Boulder Atmospheric Observatory (BAO), a national facility for remote-sensor calibration and atmospheric boundary-layer experiments, supported jointly by NOAA's Wave Propagation Laboratory and the National Center for Atmospheric Research, was completed. The facility features a 300 m meteorological tower instrumented at eight levels (10, 22, 50, 100, 150, 200, 250 and 300 m height) plus a movable carriage for measuring height profiles. Three-axis sonic anemometers are installed at each level on the tower. A 450 m optical crosswind triangle permanently surrounds the tower for boundary-layer convergence studies at heights of 3–4 m above the terrain.

A major field study, named PHOENIX, was carried out at the BAO during September 1978. The experiments included tests, evaluations, and comparisons of a number of remote-sensing systems. They also provided a relatively complete data set on the convectively-active planetary boundary layer (PBL) and a wide variety of atmospheric processes at work within it. One purpose of these experiments was to determine the effect of irregular terrain on the optical measurements of horizontal wind and convergence. The optically measured results were compared with wind velocity measured on the tower and with nearby surface anemometers.

2. Instrumentation

The convergence triangle at the BAO uses a more sophisticated incoherent, extended-aperture, optical wind system than the laser wind system used by Kjelaas and Ochs (1974). Its use of incoherent light and 15 cm apertures essentially eliminates any chance of bias caused by strong turbulence

[1] *Visiting scientist with Wave Propagation Laboratory during 1978–1979.* Permanent affiliation: Department of Production Engineering, College of Science, National Central University, Chung-li, Taiwan, Republic of China.

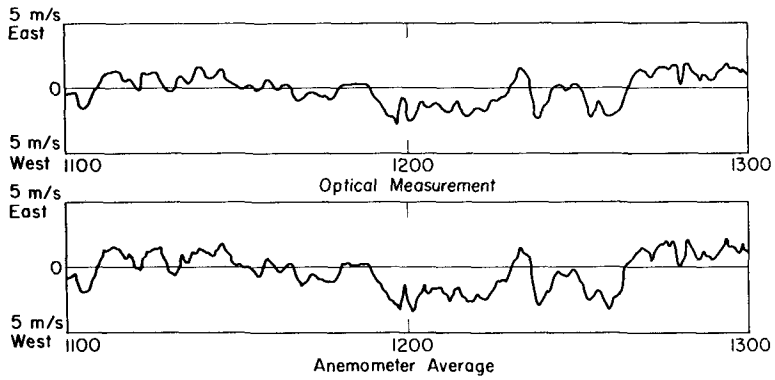

FIG. 1. Comparison of the saturation-resistant system measurement of wind with the average of measurements of five anemometers that read the horizontal crosswind component in the middle third of the optical path.

(the so-called "saturation effect"; see details by Ochs *et al.*, 1976) over the 450 m line-of-sight path. The new system is also insensitive to changes in the inner and outer scale lengths of the refractive turbulence (Wang *et al.*, 1978). A detailed description of the system is beyond the scope of this paper; it will be given in a future paper. The system was tested on a 500 m optical path instrumented with ten anemometers aligned to measure the horizontal crosswind component. The optical system measures the wind predominantly in the middle third of the path (Ochs *et al.*, 1976). A comparison of the optical system measurement with the average of five anemometers reading the horizontal crosswind component in the middle third of the optical path is shown in Fig. 1. The agreement is excellent even for detailed variations.

Three similar optical systems 3–4 m above the ground were used to form a 450 m equilateral triangle around the 300 m tower. Wind readings from the optical system and from the anemometers at each tower level were averaged over 10 s by a minicomputer at the tower base and brought to the Boulder Laboratory for processing.

3. Convergence Measurements

Fig. 2 shows the location of the optical triangle relative to the meteorological tower and to nearby Portable Automated Mesonet (PAM) stations provided and operated by the National Center for Atmospheric Research. The PAM system (Brock and Govind, 1977) consists of a network of remote meteorological ground stations (monitoring wind speed and direction, pressure, temperature, humidity and other parameters) which transmit data by radio to a base station for recording. The terrain is relatively flat inside the triangle and slightly irregular outside. The tower is in the middle of the optical triangle. Because each optical path was arranged to read an outflowing wind as positive, the sum of the readings of all three paths represents the horizontal wind divergence, i.e.,

$$\nabla_h \cdot \mathbf{V} = L(V_N + V_{SE} + V_{SW})A^{-1}, \quad (1)$$

where V_N, V_{SE}, and V_{SW} are the wind components (m s^{-1}) transverse to the north, southeast and southwest triangle sides, respectively; L is the side of the triangle; and A is the area of the triangle. It should be noted that the north side of the triangle is not exactly parallel to the east-west direction. For a 450 m equilateral triangle, Eq. (1) becomes

$$\nabla_h \cdot \mathbf{V} = 5.128 \times 10^{-3}\,(V_N + V_{SE} + V_{SW}), \quad (2)$$

where the divergence is in s^{-1}. The vertical wind velocity is related to the divergence field through the equation of continuity as

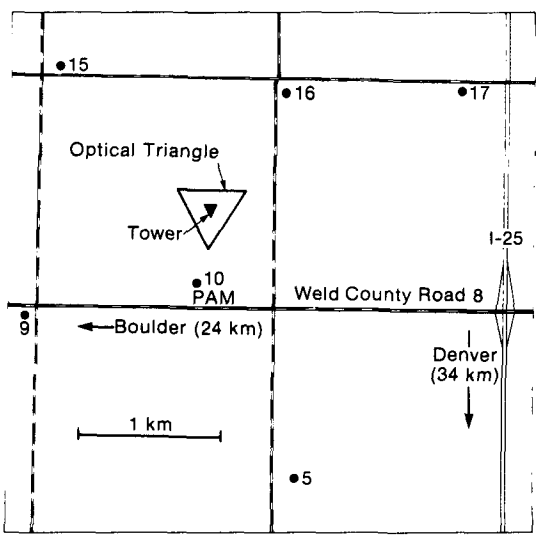

FIG. 2. Map showing location of the optical triangle relative to the meteorological tower and the nearby Portable Automated Mesonet (PAM) stations.

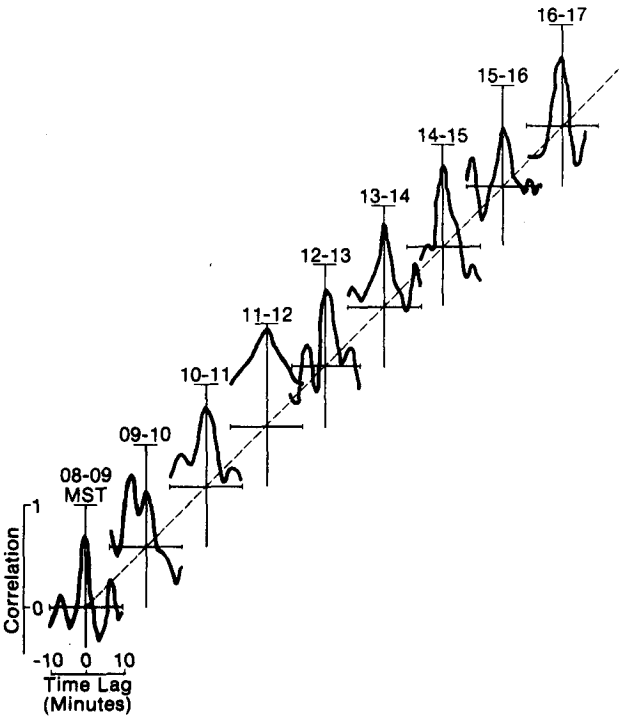

FIG. 3. Time-sequence samples of the hourly averaged time-lagged correlations of the vertical wind measured at 100 m above the ground and the optically measured convergence near the ground during daytime when convective plumes are active. Running averages of 100 s were used to suppress the contribution from small plumes.

$$W(z) = -\int_0^z dz \nabla_h \cdot \mathbf{V}(z), \qquad (3)$$

where $W(z)$ denotes the vertical wind velocity at height z. Because the optical measurements are made near the ground, their cross correlation with the vertical wind at different heights on the tower indicates how high the vertical wind can be inferred by measuring the ground-level horizontal convergence. Typical samples of the hourly averaged time-lagged correlations of the vertical wind measured at 100 m above the ground and the optically measured convergence near the ground during daytime are shown in Fig. 3. In calculating the cross correlations, a 100 s running average was used to suppress the contributions from small scale plumes. Because the tower was outside the triangle in the experiment reported by Kjelaas and Ochs (1974), the peak in their cross correlations did not occur at zero lag but was shifted in time by the amount of travel time between the tower and the center of the triangle. In our case the tower is in the center of the optical triangle and the peaks of the cross correlations are usually very close to zero delay especially when high correlations are present. This indicates that the plumes were not tilted.

A contour plot of the peak value of the correlation is shown in Fig. 4. Because small-scale plumes contribute the most to the low-altitude vertical winds, the correlations are not good for the two lowest levels. The correlations are usually good for wind measured at 50 m or higher, especially during strong convective activities. From the correlation analysis, the inversion layer height can be identified as being below 300 m, if the correlation is found to reach a maximum at levels below the top of the tower, and fall to relatively low values at 300 m.

A combination measurement of the inversion layer base was performed on 21 September 1978, by various remote sensors (e.g., FM-CW radar,

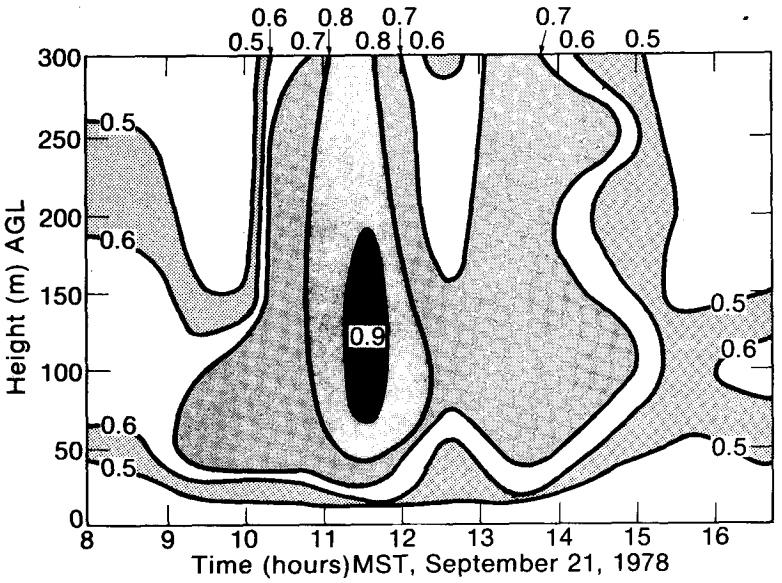

FIG. 4. A height-time contour plot of the peak value of the cross-correlation between the vertical wind and the horizontal divergence.

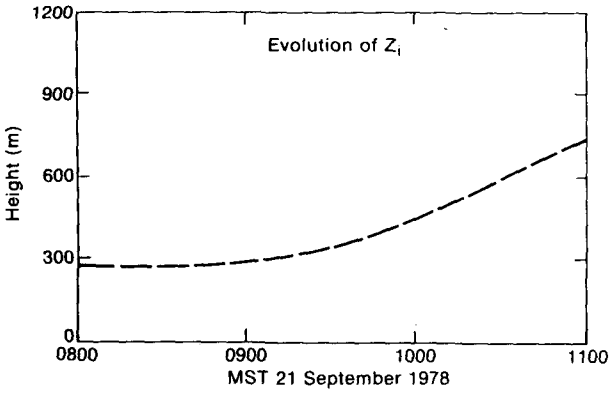

FIG. 5. Best fit curve through estimates of Z_i (height of lowest inversion base) from BAO tower, aircraft, lidar, FM-CW radar, X-band radar, and 8 mm radar.

lidar, X-band radar, 8 mm radar and acoustic sounder). The results are shown in Fig. 5. During early hours in the morning, the inversion layer is low. Between 0800 and 0900, the measured inversion height is between 250 and 300 m. This was also indicated by the cross correlation between the optical convergence measurement and the tower vertical wind measurements (Fig. 4). During this period, the correlations are highest below the inversion layer. Moreover, the correlation is lowest for the 300 m data which were measured above the inversion layer. The detailed variations of the optically measured convergences and the vertical winds at 100 and 300 m heights during this period are shown in Fig. 6. It clearly indicates that the horizontal convergences measured close to the ground follow the vertical winds at 100 m (below the inversion layer) better than at 300 m (above the inversion layer). The normalized correlation coefficient is 0.64 for 100 m data, and is only 0.21 for 300 m data, which is close to the correlation noise level induced by small scale plumes for a 100 s running average. To suppress the contributions from small-scale plumes even more, we calculated the correlation using a 300 s running average. The results show that the correlations are 0.72 and 0.04 at 100 and 300 m, respectively. The inversion height started to move up at 0900 and was higher than 400 m after 1000. The correlations are then high up to at least 300 m while convection was active.

4. Horizontal wind vector

The optical triangle measures the averaged horizontal wind vectors over its area. By elementary geometry, it can be shown that

$$\bar{V}_E = 0.5(V_{SE} - V_{SW})/\cos 30^\circ, \quad (4)$$

$$\bar{V}_N = [2V_N - (V_{SE} + V_{SW})]/3, \quad (5)$$

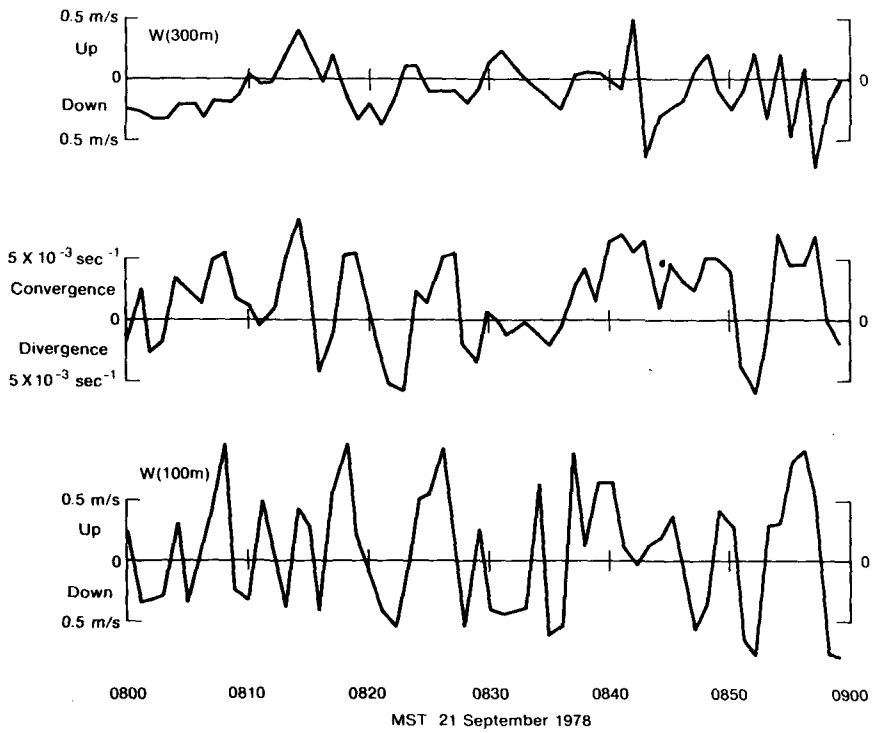

FIG. 6. The temporal variations of the optically measured convergence (middle curve) and the vertical winds at 100 and 300 m. The horizontal convergence follows the vertical wind at 100 m (below the inversion layer) better than at 300 m (above the inversion layer).

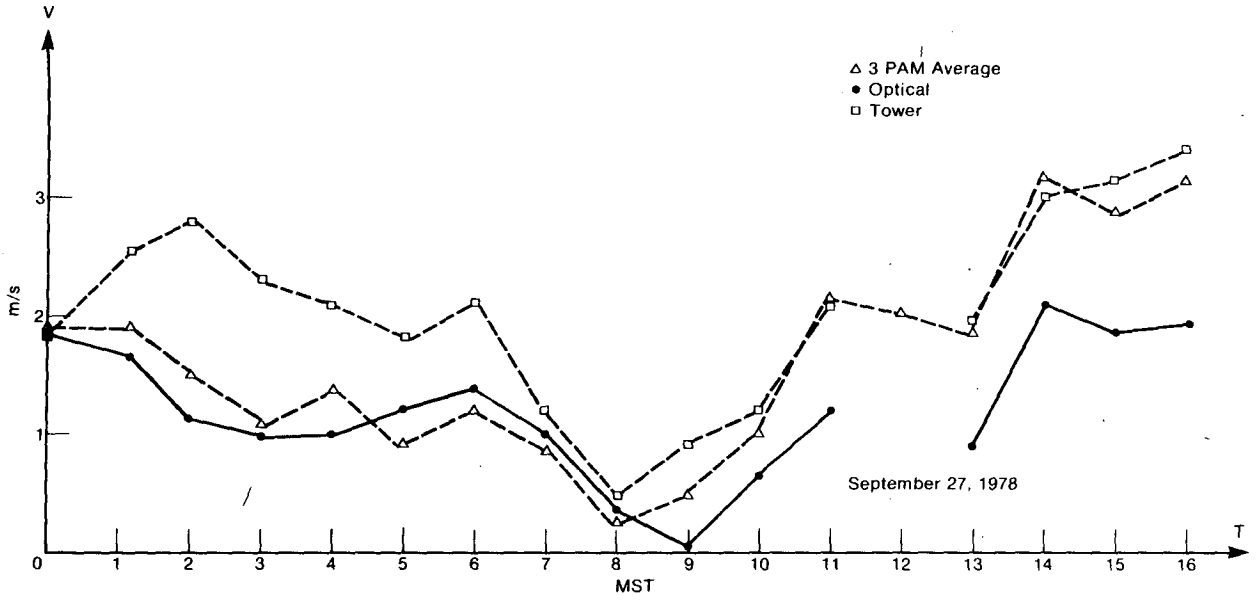

FIG. 7. The horizontal wind speeds measured by the optical triangle, the tower anemometers (10 m), and the average of three nearby PAM stations.

where $\bar{V}_E$ and $\bar{V}_N$ denote the wind components, averaged over all three sides of the triangle, toward east and north, respectively. The wind components measured by Eqs. (4) and (5) represent the averages over the whole triangle. This can be seen from rewriting Eq. (5) as

$$\bar{V}_N = V_N - (V_N + V_{SE} + V_{SW})/3. \quad (6)$$

When there is a uniform wind over the whole area, the second term in Eq. (6) is zero, hence $\bar{V}_N = V_N$. However, if the net divergence over the triangle is not zero, $\bar{V}_N$ is no longer equal to V_N. This could be seen clearly if we assume that the mean wind is zero (which implies $\bar{V}_N = 0$), and $V_N = V_{SE} = V_{SW} = \epsilon$. If we use Eq. (6), $\bar{V}_N = 0$, while $V_N = \epsilon \neq 0$. The wind speed and direction can be obtained by

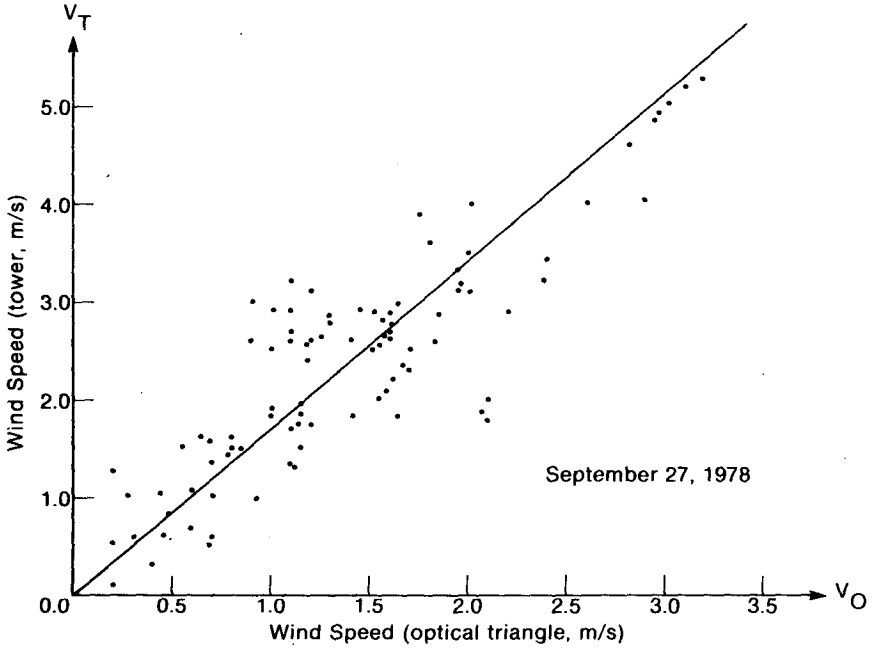

FIG. 8. A scatter diagram of the wind speeds measured by the optical triangle and by the tower anemometers (10 m).

$$\bar{V} = (\bar{V}_E^2 + \bar{V}_N^2)^{1/2}, \quad (7)$$

$$\theta = \tan^{-1} \frac{\bar{V}_E}{\bar{V}_N} + 180° + 4°, \quad (8)$$

where θ is the azimuth angle (measured clockwise from north) from which the wind is blowing. The extra correction of 4° is needed because the north side of the triangle is not exactly parallel to the east-west direction.

We compared the horizontal wind vectors obtained from the optical triangle with the lowest level (10 m) measurements from the tower. The results are shown in Fig. 7. Because the tower data were measured at a higher altitude (10 m) than the optical measurements (3 m), the tower-measured wind speeds are always stronger than the optically measured speeds. A scatter diagram of the two measurements is shown in Fig. 8. There is a linear relationship (indicated by the solid line) between the two measurements, although the data are somewhat scattered. The average of speeds measured by the three nearby PAM (Portable Automated Mesonet) stations (station #10, #15, and #16, see Fig. 3) is also shown in Fig. 7 for comparison. The general agreement is good.

A comparison of the wind directions measured by the tower instruments at 10 m and the optical triangle, and the average of wind directions measured at three nearby PAM stations (4 m height) is shown in the upper diagram of Fig. 9. A scatter diagram of the tower measurements versus optical measurements is shown in Fig. 10. The agreement is good though not perfect. To test the spatial

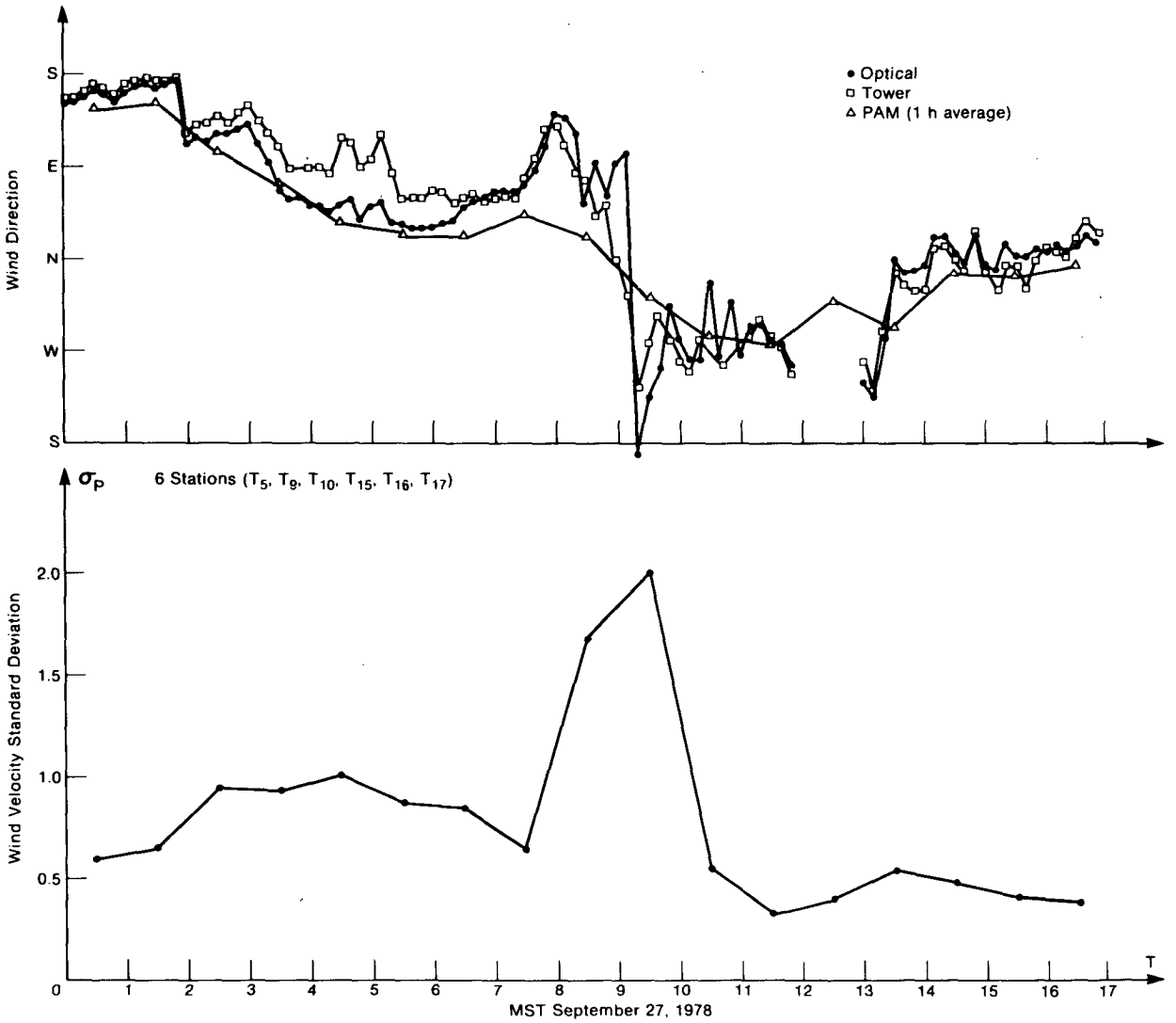

FIG. 9. A comparison of the wind directions measured by tower instruments (10 m level), the optical triangle, and three nearby PAM stations (upper diagram). The standard deviation σ of the velocities measured by six nearby PAM stations is shown in the lower diagram.

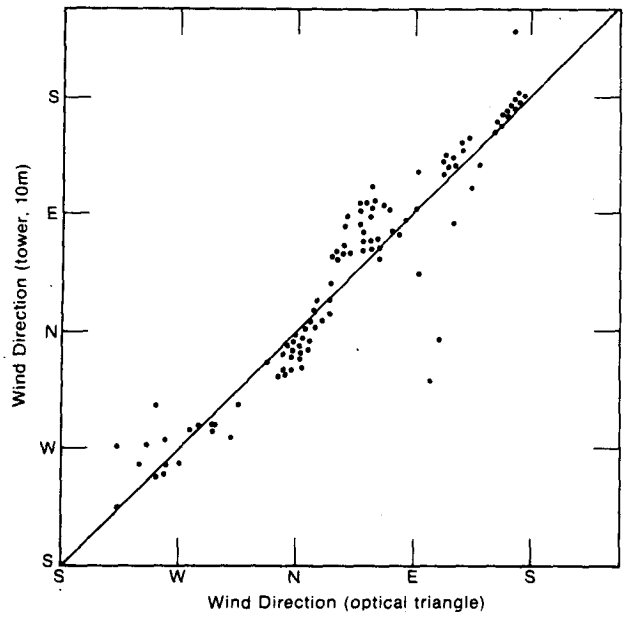

FIG. 10. A scatter diagram of the tower measurements (10 m) versus optical measurements of the horizontal wind directions.

variation of the wind velocities, we determined the normalized standard deviation σ of the velocities measured by six nearby PAM stations (#5, 9, 10, 15, 16, 17, see Fig. 2), which is given by

$$\sigma^2 = (\sigma_E^2 + \sigma_N^2)/\bar{V}^2, \quad (9)$$

where σ_E and σ_N are the standard deviations of the east-west and north-south wind components respectively. The result is shown in the lower diagram of Fig. 9. It is clear that the difference between the tower and the optical data becomes significant when the spatial variation of wind velocity is large ($\sigma > 0.7$).

To show the effect of the irregular terrain, the optically measured convergence as a function of the horizontal wind direction is plotted in Fig. 11. Data from nine days are included. The dots indicate the 20 min averages during daytime (0800–1700) when convective plumes are active. We divided the direction axis into twelve 30° sectors. The average of the data points in each sector is shown by the triangle. The wind direction bias seen in Fig. 11 is consistent with what would be expected from differences in the height above ground for the three optical paths. Although the pillars at the corners are at identical heights, the measured heights above ground for the center of the optical paths are 3.5 m for V_N, 2.6 m for V_{SE}, and 3.3 m for V_{SW}. Since surface friction causes wind to be less near the ground, one would expect $V_N + V_{SE} + V_{SW}$ to be biased toward positive (divergent) for a southeast wind and toward negative (convergent) for a northwest wind, and that is what we observe. In addition to the directional dependence, the data are also offset toward divergence, which could be an effect of irregular terrain.

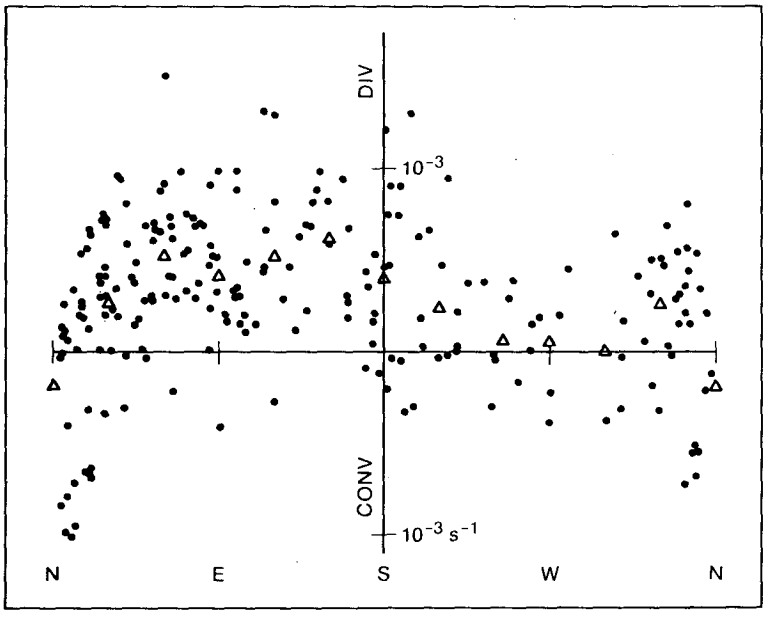

FIG. 11. Optically measured horizontal convergence as a function of the horizontal wind direction. The dots indicate the 20 min averages during daytime (0800–1700) when convective plumes are active. The triangles denote the averages of the data points in 30° sectors.

5. Conclusions

The convergence measured by three sets of optical wind sensors that form a triangle near the ground is proportional to the vertical wind in the middle of the triangle up to at least 300 m during convective activity even for slightly irregular terrain. The space-averaged horizontal wind velocities can be obtained from the wind measurements of the three sides of the triangle. These space-averaged measurements are more representative of the average wind than a few instruments *in situ* can be. Because the optical instruments can accurately measure the space-averaged wind velocities, the effect of the irregular terrain can clearly be observed.

Acknowledgments. The authors are indebted to Dr. J. C. Kaimal for many suggestions and valuable discussions. We would also like to thank Dr. P. H. Hildebrand of the National Center for Atmospheric Research for providing the PAM data. The senior author expresses his sincere gratitude to Dr. C. Gordon Little, Director of the Wave Propagation Laboratory, and to the National Science Council, Taipei, Taiwan, Republic of China, for providing him with the opportunity to make this study while on leave from the National Central University, Chung-li, Taiwan, Republic of China.

REFERENCES

Bellamy, J. C., 1949: Objective calculations of divergence, vertical velocity and vorticity. *Bull. Amer. Meteor. Soc.*, **30**, 45–49.

Brock, F. V., and P. K. Govind, 1977: Portable Automated Mesonet in operation. *J. Appl. Meteor.*, **16**, 299–310.

Eddy, A., 1964: The objective analysis of horizontal wind divergence fields. *Quart. J. Roy. Meteor. Soc.*, **90**, 424–440.

Endlich, R. M., and J. R. Clark, 1963: Objective computations of some meteorological quantities. *J. Appl. Meteor.*, **2**, 66–81.

Kjelaas, A. G., and G. R. Ochs, 1974: Study of divergence in the boundary layer using optical propagation techniques. *J. Appl. Meteor.*, **13**, 242–248.

Morton, B. R., G. I. Taylor and J. W. Turner, 1956: Turbulent gravitational convection from maintained and instantaneous sources. *Proc. Roy. Soc. London*, **A234**, 1–23.

Ochs, G. R., S. F. Clifford, and Ting-i Wang, 1976: Laser wind sensing: the effects of saturation of scintillation. *Appl. Opt.*, **15**, 403–408.

Telford, J. W., 1966: The convective mechanisms in clear air. *J. Atmos. Sci.*, **23**, 652–666.

Wang, Ting-i, G. R. Ochs, and S. F. Clifford, 1978: A saturation-resistant optical scintillometer to measure C_n^2. *J. Opt. Soc. Amer.*, **68**, 334–338.